Wavlet analysis of covariance with application to atmospheric time series

Brandon Whichter Peter Guttorp Donald Percival

NRCSE

Technical Report Series

NRCSE-TRS No. 024

Wavelet analysis of covariance with application to atmospheric time series

Brandon Whitcher
EURANDOM, P.O. Box 513, 5600 MB Eindhoven, The Netherlands.

Peter Guttorp
University of Washington, Department of Statistics, Box 354322, Seattle, WA 98195-4322, USA.

Donald B. Percival
University of Washington, Applied Physics Laboratory, Box 355640, Seattle, WA 98195-5640, USA; and MathSoft, Inc., 1700 Westlake Avenue North, Seattle, Washington 98109-9891, USA.

Short title:

Abstract. Multi-scale analysis of univariate time series has appeared in the literature at an ever increasing rate. Here we introduce the multi-scale analysis of covariance between two time series using the discrete wavelet transform. The wavelet covariance and wavelet correlation are defined and applied to this problem as an alternative to traditional cross-spectrum analysis. The wavelet covariance is shown to decompose the covariance between two stationary processes on a scale by scale basis. Asymptotic normality is established for estimators of the wavelet covariance and correlation. Both quantities are generalized into the wavelet cross-covariance and cross-correlation in order to investigate possible lead/lag relationships. A thorough analysis of El-Niño–Southern Oscillation events and the Madden–Julian oscillation is performed using a 35+ year record. We show how potentially complicated patterns of cross-correlation are easily decomposed using the wavelet cross-correlation on a scale by scale basis, where each wavelet cross-correlation series is associated with a specific physical time scale.

Some key words: Confidence intervals; Cross-correlation; Cross-covariance; Madden–Julian oscillation; Maximal overlap discrete wavelet transform; Southern Oscillation Index.

1. Introduction

The bivariate relationship between two time series is often of crucial interest in atmospheric science. For example, the Madden–Julian oscillation (MJO) [*Madden and Julian*, 1971] was found using bivariate spectral analysis between the station pressure and zonal wind components at Canton Island (2.8°S, 171.7°W) – specifically the co-spectrum and magnitude squared coherence. This oscillation has been documented as having a period anywhere from 30–60 days and has appeared in many studies in the Indian Ocean and tropical Pacific Ocean; see *Madden and Julian* [1994] for a review. This apparent broadband nature of the oscillation has been hypothesized as being nonstationary, so the broad peak observed in previous spectral analyses might be attributed to the fading in-and-out of the oscillation over the measured time series. Temporal variations in the MJO and its relationship with El Niño–Southern Oscillation (ENSO) events have previously been investigated using traditional cross-spectral analysis.

Given the nonstationary nature of the MJO, analyzing it through a transform which captures events both locally in time and frequency is appealing. The short-time Fourier transform is one such technique, where the discrete Fourier transform is applied to subsets of the time series via a moving window resulting in a grid-like partition of the time-frequency plane. The discrete wavelet transform (DWT) is another technique, where the time-frequency plane is partitioned such that high-frequencies are given small windows in time and low-frequencies are given large windows in time via an adaptive windowing of the time series. See *Kumar and Foufoula-Georgiou* [1994] and *Kumar* [1996] for descriptions of time-frequency/time-scale analysis. An non-decimated version of the orthonormal DWT – the maximal overlap DWT (MODWT) – has proven useful in analyzing various geophysical processes [*Percival and Guttorp*, 1994; *Percival and Mofjeld*, 1997].

In this paper, we deal with a formulation of the wavelet covariance and correlation

between two time series based upon the MODWT and Daubechies family of wavelets with compact support [*Daubechies*, 1992, Sec. 6.2]. We show that the wavelet covariance offers a scale by scale decomposition of the usual covariance between time series. We then derive statistical properties of estimators of the wavelet covariance and correlation. Both quantities are generalized into the wavelet cross-covariance and cross-correlation in order to investigate possible lead/lag relationships. We demonstrate the use of these results in an analysis of the relationship between a Southern Oscillation Index (SOI) time series and the station pressure series from Truk Island (7.4°N, 151.8°W).

1.1. Relationship to Previous Work

Previous work on the time-varying nature of the MJO includes *Anderson* et al. [1984] who filtered atmospheric relative angular momentum (4 years) and the 850–200 mb shear of the zonal wind at Truk Island (25 years) with a filter designed to pass the frequency band corresponding to periods of 32–64 days. They noted that, with respect to the Truk Island series, a possible association with increased amplitude of the oscillation during the 1956–57, 1972–73, and 1976–77 ENSO warm events but noted that the duration of these increases were much longer than the ENSO events. *Madden* [1986] performed a seasonally varying cross-spectral analysis on nearly twenty time series of rawinsonde data from tropical stations around the world. The MJO appears strongest during December–February and weakest during June–August, and that it is always stronger in the western Pacific and Indian oceans than elsewhere. *Madden and Julian* [1994] note the broadband nature of the oscillation by comparing the station pressure spectra for Truk Island (7.4°N, 151.8°W) during two time spans – 1967 to 1979 and 1980 to 1985. The MJO appears to have a 26-day period in the early 1980s.

The influence of ENSO events has also been hypothesized to affect the period of the MJO. *Gray* [1988] performed a correlation analysis between daily station pressure data from Truk (7°N, 152°W), Balboa (9°N, 80°W), Darwin (12°S, 131°E) and Gan

(1°S, 73°E), with seasonal sea surface temperature anomalies on a 5° grid. The data were partitioned into ENSO and non-ENSO years; in non-ENSO years a strong seasonal shift in frequency was found at all sites except Truk Island. *Kuhnel* [1989] investigated the characteristics of a 40–50 day oscillation in cloudiness for the Australo–Indonesian region. Using data on a 10° by 5° grid, regions in the eastern Indian Ocean and western Pacific Ocean were found to have a pronounced 40–50 day peak with no obvious seasonal variation. Another region in the Indian Ocean (5–15°S, 95–100°E) showed a stronger oscillation in the March–June period. Regions around 5–15°S over northern Australia and in the Pacific Ocean showed a much stronger 40–50 day oscillation during the Australian monsoon season from December to March, than the rest of the year. The 40–50 day cloud amount oscillation did not appear to be affected by warm ENSO events.

The ability of the DWT to capture variability in both time and scale can provide insight into the nature of atmospheric phenomena such as the MJO, but we must make use of the DWTs of two time series in such a way that these bivariate properties can be brought out. *Hudgins* [1992] introduced the concepts of the wavelet cross spectrum and wavelet cross correlation in his thesis, both in terms of the continuous wavelet transform (CWT). In a subsequent paper, *Hudgins* et al. [1993] applied these concepts to atmospheric turbulence. They found the bivariate wavelet techniques provided a better analysis of the data over traditional Fourier methods – especially at low frequencies. *Liu* [1994] defined a cross wavelet spectrum, equivalent to that of *Hudgins* [1992], and complex-valued wavelet coherency which was constructed using the co- and quadrature wavelet spectra. These quantities were used to reveal new insights on ocean wind waves; such as wave group parameterizations, phase relations, and wave breaking characteristics. *Lindsay* et al. [1996] defined the sample wavelet covariance for the DWT and MODWT along with confidence intervals based on large sample results. They applied this methodology to the surface temperature and albedo of ice pack in the Beaufort Sea. Recently, *Torrence and Compo* [1998] discussed the cross-wavelet

spectrum, which is complex valued, and the cross-wavelet power, which is the magnitude of their cross-wavelet spectrum, in terms of the CWT. They also introduced confidence intervals for their cross-wavelet power and compared the SOI with Niño3 sea surface temperature readings.

In this paper, we extend the notion of wavelet covariance for the MODWT and define the wavelet cross-covariance and wavelet cross-correlation. The wavelet cross-covariance is shown to decompose the process cross-covariance on a scale by scale basis for specific types of nonstationary stochastic processes. Asymptotic normality is proven for the MODWT-based estimators of wavelet cross-covariance.

1.2. Outline

The MODWT, a non-decimated variation of the DWT, is described in Section 2. In Section 3, the wavelet cross-covariance and cross-correlation are defined in terms of the MODWT coefficients at a particular scale of the transform. Central limit theorems are stated for estimators of both quantities based on a finite sample of MODWT coefficients (proofs are given in the Appendix). Explicit methods for computing approximate $100(1-2p)\%$ confidence intervals are provided in Section 4. Fisher's z-transformation is utilized in order to keep the confidence interval of the wavelet correlation bounded by ± 1 for small sample sizes.

In Section 5, we perform a wavelet analysis of covariance with a daily Southern Oscillation Index and daily station pressure readings from Truk Island. Spectral analysis shows two peaks in the magnitude squared coherence between the two time series around the established MJO range of frequencies, and cross-correlation analysis provides a complicated correlation structure. The wavelet cross-correlation decomposes the usual cross-correlation producing several patterns associated with physical time scales. Using the wavelet cross-correlation, the relationship between the two time series is more easily shown.

2. Maximal Overlap Discrete Wavelet Transform

The DWT of a time series $\mathbf{X}$ is now a reasonably well-established method for analyzing its multi-scale features. In this section we provide a brief introduction to a slight variation of the DWT, called the maximal overlap DWT (MODWT). The MODWT gives up orthogonality (through not subsampling) in order to gain features such as translation-invariance and the ability to analyze any sample size. Here, we follow previous definitions of the MODWT by *Percival and Guttorp* [1994] and *Percival and Mofjeld* [1997].

Let $\{\tilde{h}_1\} \equiv \{\tilde{h}_{1,0}, \ldots, \tilde{h}_{1,L-1}\}$ denote a the wavelet filter coefficients from a Daubechies compactly supported wavelet family [*Daubechies*, 1992, Sec. 6.2] and let $\{\tilde{g}_1\} \equiv \{\tilde{g}_{1,0}, \ldots, \tilde{g}_{1,L-1}\}$ be the corresponding scaling filter coefficients, defined via the following quadrature mirror relationship $\tilde{g}_{1,m} = (-1)^{m+1}\tilde{h}_{1,L-1-m}$. By definition, the wavelet filter $\{\tilde{h}_1\}$ is associated with unit scale, is normalized such that $\sum \tilde{h}_l^2 = 1/2$ and is orthogonal to its even shifts. For any sample size $N \geq L$ and with $h_{1,m} = 0$ for $m \geq L$, let

$$\widetilde{H}_{1,k} = \sum_{m=0}^{N-1} \tilde{h}_{1,m}\, e^{-i2\pi mk/N}, \quad k = 0, \ldots, N-1,$$

be the discrete Fourier transform (DFT) of $\{\tilde{h}_1\}$, and let $\widetilde{G}_{1,k}$ denote the DFT of $\{\tilde{g}_1\}$. Now define the wavelet filter $\{\tilde{h}_j\}$ for scale $\lambda_j \equiv 2^{j-1}$ as the inverse DFT of

$$\widetilde{H}_{j,k} = \widetilde{H}_{1,2^{j-1}k \bmod N} \prod_{l=0}^{j-2} \widetilde{G}_{1,2^l k \bmod N}, \quad k = 0, \ldots, N-1.$$

The wavelet filter associated with scale λ_j has length $\min\{N, L_j\}$ where $L_j \equiv (2^j - 1)(L-1) + 1$. When $N > L_j$, define $\tilde{h}_{j,m} = 0$ for $m \geq L_j$. Also, define the scaling filter $\{\tilde{g}_J\}$ for scale $2\lambda_J$ as the inverse DFT of

$$\widetilde{G}_{J,k} = \prod_{l=0}^{J-1} \widetilde{G}_{1,2^l k \bmod N}, \quad k = 0, \ldots, N-1.$$

In order to construct a jth order partial MODWT, we let $\{\mathcal{X}_k\} \equiv \{\mathcal{X}_0, \ldots, \mathcal{X}_{N-1}\}$ be the DFT of $\mathbf{X}$ (for arbitrary N). The vector of MODWT coefficients $\widetilde{\mathbf{W}}_j$, $j = 1, \ldots, J$ is defined to be the inverse DFT of $\{\widetilde{H}_{j,k}\mathcal{X}_k\}$ and is associated with changes of scale λ_j. The vector of MODWT scaling coefficients $\widetilde{\mathbf{V}}_J$ is defined similarly by the inverse DFT of $\{\widetilde{G}_{J,k}\mathcal{X}_k\}$ and is associated with averages of scale $2\lambda_J$ and higher. For time series of dyadic length, the MODWT may be subsampled and rescaled to obtain an orthonormal DWT. In practice, a pyramid scheme similar to that of the DWT is utilized to compute the MODWT; see *Percival and Guttorp* [1994] and *Percival and Mofjeld* [1997].

Percival and Mofjeld [1997] proved that the MODWT is an energy preserving transform in the sense that

$$\|\mathbf{X}\|^2 = \sum_{j=1}^{J} \left\|\widetilde{\mathbf{W}}_j\right\|^2 + \left\|\widetilde{\mathbf{V}}_J\right\|^2.$$

This allows for a scale-based analysis of variance of a time series similar to spectral analysis via the DFT. In a wavelet analysis of variance, the individual wavelet coefficients are associated with a band of frequencies and specific time scale whereas Fourier coefficients are associated with a specific frequency only.

3. Wavelet-Based Estimators of Covariance and Correlation

Here we define the basic quantities of interest for estimating association between two time series using the MODWT. The decomposition of covariance on a scale by scale basis of the wavelet covariance is shown, and central limit theorems are provided for the wavelet covariance and correlation.

3.1. Definition and Properties of the Wavelet Cross-Covariance

Let $\{U_t\} \equiv \{\ldots, U_{-1}, U_0, U_1, \ldots\}$ be a stochastic process whose dth order backward difference $(1-B)^d U_t = Z_t$ is a stationary Gaussian process with zero mean and spectral

density function $S_Z(\cdot)$, where d is a non-negative integer. Let

$$\overline{W}_{j,t}^{(U)} = \tilde{h}_{j,l} * U_t \equiv \sum_{l=0}^{L_j-1} \tilde{h}_{j,l} U_{t-l}, \quad t = \ldots, -1, 0, 1, \ldots,$$

be the stochastic process obtained by filtering $\{U_t\}$ with the MODWT wavelet filter $\{\tilde{h}_{j,l}\}$. *Percival and Walden* [1999, Sec. 8.2] showed that if $L \geq 2d$, then $\{\overline{W}_{j,t}^{(U)}\}$ is a stationary process with zero mean and spectrum given by $S_{j,U}(\cdot)$.

Let $\{X_t\} \equiv \{\ldots, X_{-1}, X_0, X_1, \ldots\}$ and $\{Y_t\} \equiv \{\ldots, Y_{-1}, Y_0, Y_1, \ldots\}$ be stochastic processes whose d_Xth and d_Yth order backward differences are stationary Gaussian processes as defined above, and define $d \equiv \max\{d_X, d_Y\}$. Let $S_{XY}(\cdot)$ denote their cross spectrum and, $S_X(\cdot)$ and $S_Y(\cdot)$ denote their autospectra, respectively. The cross spectrum is a complex valued function defined to be $S_{XY}(f) \equiv \sum_{\tau=-\infty}^{\infty} C_{\tau,XY} e^{-i2\pi f\tau}$ for $|f| \leq 1/2$, where $C_{\tau,XY}$ is the cross covariance sequence given by $C_{\tau,XY} \equiv \mathrm{Cov}\{X_t, Y_{t+\tau}\}$. The wavelet cross-covariance of $\{X_t, Y_t\}$ for scale $\lambda_j = 2^{j-1}$ and lag τ is defined to be

$$\gamma_{\tau,XY}(\lambda_j) \equiv \mathrm{Cov}\left\{\overline{W}_{j,t}^{(X)}, \overline{W}_{j,t+\tau}^{(Y)}\right\}, \tag{1}$$

where $\{\overline{W}_{j,t}^{(X)}\}$ and $\{\overline{W}_{j,t}^{(Y)}\}$ are the scale λ_j MODWT coefficients for $\{X_t\}$ and $\{Y_t\}$, respectively. When $L \geq 2d$ the MODWT coefficients have mean zero and therefore $\gamma_{\tau,XY}(\lambda_j) = E\{\overline{W}_{j,t}^{(X)} \overline{W}_{j,t+\tau}^{(Y)}\}$. By setting $\tau = 0$ and Y_t to X_t or X_t to Y_t, Equation (1) reduces to the wavelet variance for X_t or Y_t denoted as, respectively, $\nu_X^2(\lambda_j)$ or $\nu_Y^2(\lambda_j)$ [*Percival*, 1995].

The following theorem demonstrates that the wavelet cross-covariance decomposes the covariance between two stationary time series on a scale by scale basis.

Theorem 1 *Let $\{X_t\}$ and $\{Y_t\}$ be weakly stationary processes with autospectra $S_X(\cdot)$ and $S_Y(\cdot)$, respectively. Let $L > 2d$ and define $\overline{V}_{J,t}^{(X)} \equiv \tilde{g}_{J,l} * X_t$ and $\overline{V}_{J,t}^{(Y)} \equiv \tilde{g}_{J,l} * Y_t$, which are stationary processes obtained by filtering $\{X_t\}$ and $\{Y_t\}$ using the MODWT scaling filter $\{\tilde{g}_{J,l}\}$, respectively. For any integer $J \geq 1$, we have*

$$C_{\tau,XY} = \mathrm{Cov}\{X_t, Y_{t+\tau}\} = \mathrm{Cov}\left\{\overline{V}_{J,t}^{(X)}, \overline{V}_{J,t+\tau}^{(Y)}\right\} + \sum_{j=1}^{J} \gamma_{\tau,XY}(\lambda_j).$$

As $J \to \infty$, we have $C_{\tau,XY} = \sum_{j=1}^{\infty} \gamma_{\tau,XY}(\lambda_j)$, that is, the wavelet cross-covariance decomposes the cross-covariance between $\{X_t\}$ and $\{Y_t\}$ on a scale by scale basis.

If we think of $\{\tilde{g}_J\}$ as a low-pass filter covering the nominal band $[-2^{-(J+1)}, 2^{-(J+1)}]$, this statement is intuitively plausible since the scaling filter $\{\tilde{g}_J\}$ is capturing smaller and smaller portions of the cross spectrum as $J \to \infty$.

3.2. Estimating the Wavelet Cross-Covariance

Suppose $X_0, \ldots, X_{N-1}$ and $Y_0, \ldots, Y_{N-1}$ can be regarded as realizations of portions of the processes $\{X_t\}$ and $\{Y_t\}$, whose d_Xth and d_Yth order backward differences form stationary Gaussian processes. As before, let $d = \max\{d_X, d_Y\}$.

Let $\widetilde{W}_{j,t} = \overline{W}_{j,t}$ for those indices t where $\widetilde{W}_{j,t}$ is unaffected by the boundary – this is true as long as $t \geq L_j - 1$. Thus, if $N \geq L_j$, we can define a biased estimator $\tilde{\gamma}_{\tau,XY}(\lambda_j)$ of the wavelet cross-covariance based upon the MODWT via

$$\tilde{\gamma}_{\tau,XY}(\lambda_j) \equiv \begin{cases} \widetilde{N}_j^{-1} \sum_{l=L_j-1}^{N-\tau-1} \widetilde{W}_{j,l}^{(X)} \widetilde{W}_{j,l+\tau}^{(Y)}, & \tau = 0, \ldots, \widetilde{N}_j - 1; \\ \widetilde{N}_j^{-1} \sum_{l=L_j-1-\tau}^{N-1} \widetilde{W}_{j,l}^{(X)} \widetilde{W}_{j,l+\tau}^{(Y)}, & \tau = -1, \ldots, -(\widetilde{N}_j - 1); \\ 0, & \text{otherwise}, \end{cases}$$

where $\widetilde{N}_j \equiv N - L_j + 1$. The bias is due to the denominator $1/\widetilde{N}_j$ remaining constant for all lags, though it disappears at lag $\tau = 0$. The following theorem establishes asymptotic normality for the MODWT-based estimator of the wavelet covariance. We may generalize to the wavelet cross-covariance by simply replacing shifting $\{\overline{W}_{j,t}^{(Y)}\}$ with respect to $\{\overline{W}_{j,t}^{(X)}\}$ and appealing to the same theorem (as in the proof of Thereom 1).

Theorem 2 *If $L > 2d$, and suppose $\{\overline{W}_{j,t}^{(X)}, \overline{W}_{j,t}^{(Y)}\}$ is a bivariate Gaussian stationary process with autospectra satisfying $\int_{-1/2}^{1/2} S_{j,X}^2(f) < \infty$ and $\int_{-1/2}^{1/2} S_{j,Y}^2(f) < \infty$, then the estimator $\tilde{\gamma}_{XY}(\lambda_j)$ is asymptotically normally distributed with mean $\gamma_{XY}(\lambda_j)$ and large sample variance $\widetilde{N}_j^{-1} S_{j,\tau,(XY)}(0)$. The quantity $S_{j,(XY)}(0)$ is the spectral density function for $\{\overline{W}_{j,t}^{(X)} \overline{W}_{j,t}^{(Y)}\}$ (the product of the MODWT coefficients).*

Since we are strictly interested in Gaussian processes, we can re-express the variance of the wavelet covariance (see the Appendix for details) by

$$\text{Var}\{\tilde{\gamma}_{XY}(\lambda_j)\} \approx \frac{\mathcal{V}_j}{\widetilde{N}_j}, \tag{2}$$

for large $\widetilde{N}_j$, where

$$\mathcal{V}_j \equiv S_{j,(XY)}(0) = \int_{-1/2}^{1/2} S_{j,X}(f) S_{j,Y}(f)\, df + \int_{-1/2}^{1/2} S_{j,XY}^2(f)\, df. \tag{3}$$

Note, $S_{j,XY}(\cdot)$ is the cross spectrum between two series of scale λ_j MODWT coefficients whereas $S_{j,(XY)}(\cdot)$ is the autospectrum for the product of scale λ_j MODWT coefficients. This will allow us to easily construct approximate confidence intervals for the MODWT estimator of the wavelet covariance.

3.3. Wavelet Cross-Correlation

We can define the wavelet cross-correlation for scale λ_j and lag τ as

$$\rho_{\tau,XY}(\lambda_j) \equiv \frac{\text{Cov}\left\{\overline{W}_{j,t}^{(X)}, \overline{W}_{j,t+\tau}^{(Y)}\right\}}{\left(\text{Var}\left\{\overline{W}_{j,t}^{(X)}\right\} \text{Var}\left\{\overline{W}_{j,t+\tau}^{(Y)}\right\}\right)^{1/2}} = \frac{\gamma_{\tau,XY}(\lambda_j)}{\nu_X(\lambda_j)\nu_Y(\lambda_j)}.$$

Since this is just a correlation coefficient between two random variables, $-1 \leq \rho_{\tau,XY}(\lambda_j) \leq 1$ for all τ, j. The wavelet cross-correlation is roughly analogous to its Fourier counterpart – the magnitude squared coherence – but it is related to bands of frequencies (scales). Just as the cross-correlation is used to determine lead/lag relationships between two processes, the wavelet cross-correlation will provide a lead/lag relationship on a scale by scale basis.

3.4. Estimating the Wavelet Cross-Correlation

Since the wavelet cross-correlation is simply made up of the wavelet cross-covariance for $\{X_t, Y_t\}$ and wavelet variances for $\{X_t\}$ and $\{Y_t\}$, the MODWT estimator of the

wavelet cross-correlation is simply

$$\tilde{\rho}_{\tau,XY}(\lambda_j) \equiv \frac{\tilde{\gamma}_{\tau,XY}(\lambda_j)}{\tilde{\nu}_X(\lambda_j)\tilde{\nu}_Y(\lambda_j)}, \tag{4}$$

where $\tilde{\gamma}_{\tau,XY}(\lambda_j)$ is the wavelet covariance, and $\tilde{\nu}^2_X(\lambda_j)$ and $\tilde{\nu}^2_Y(\lambda_j)$ are the wavelet variances. When $\tau = 0$ we obtain the MODWT estimator of the wavelet correlation between $\{X_t, Y_t\}$.

Large sample theory for the cross-correlation is more difficult to come by than for the cross-covariance. *Brillinger* [1979] constructed approximate confidence intervals for the auto and cross-correlation sequences of bivariate stationary time series. We use his technique to establish a central limit theorem for the MODWT estimated wavelet cross-correlation. To simplify notation the following theorem gives a central limit theorem for the wavelet correlation ($\tau = 0$) but easily generalizes to arbitrary lags.

Theorem 3 *Let $L > 2d$, and suppose $\{\overline{W}^{(X)}_{j,t}, \overline{W}^{(Y)}_{j,t}\}$ is a bivariate Gaussian stationary process with square integrable autospectra, then the MODWT estimator $\tilde{\rho}_{XY}(\lambda_j)$ of the wavelet correlation is asymptotically normally distributed with mean $\rho_{XY}(\lambda_j)$ and large sample variance given by*

$$\begin{aligned}\mathrm{Var}\{\tilde{\rho}_{XY}(\lambda_j)\} \;\approx\; \frac{1}{\widetilde{N}_j} \sum_{\tau=-(\widetilde{N}_j-1)}^{\widetilde{N}_j-1} \{\, & \rho_{\tau,X}(\lambda_j)\rho_{\tau,Y}(\lambda_j) + \rho_{\tau,XY}(\lambda_j)\rho_{\tau,YX}(\lambda_j) \\ & - 2\rho_{0,XY}(\lambda_j)[\rho_{\tau,X}(\lambda_j)\rho_{\tau,YX}(\lambda_j) + \rho_{\tau,Y}(\lambda_j)\rho_{\tau,YX}(\lambda_j)] \\ & + \rho^2_{0,XY}(\lambda_j)[\tfrac{1}{2}\rho^2_{\tau,X}(\lambda_j) + \rho^2_{\tau,XY}(\lambda_j) + \tfrac{1}{2}\rho^2_{\tau,Y}(\lambda_j)]\,\},\end{aligned}$$

where $\rho_{\tau,X}(\lambda_j) \equiv E\{\overline{W}^{(X)}_{j,t}\overline{W}^{(X)}_{j,t+|\tau|}\}/[2\lambda_j\nu^2_X(\lambda_j)]$ is the scale λ_j wavelet autocorrelation for the process $\{X_t\}$.

4. Confidence Intervals for Wavelet Estimators

With central limit theorems for both the wavelet cross-covariance and cross-correlation, we may now explicitly construct an approximate confidence interval (CI) for

the estimators. For the wavelet cross-correlation, a nonlinear transformation is utilized in order to bound it between ± 1 and reduce the computational complexity of its large sample variance. Without loss of generality, we provide the following CIs for lag $\tau = 0$. We may generalize the results presented here for arbitrary lag by simply replacing $\{\widetilde{W}_{j,t}^{(X)}\}$ and $\{\widetilde{W}_{j,t}^{(Y)}\}$ with $\{\widetilde{W}_{j,t}^{(X)}\}$ where $t = L_j + \tau - 1, ..., N-1$ and $\{\widetilde{W}_{j,t+\tau}^{(Y)}\}$ where $t = L_j - 1, ..., N - \tau - 1$ for $\tau \geq 0$, or $\{\widetilde{W}_{j,t}^{(X)}\}$ where $t = L_j - 1, ..., N + \tau - 1$ and $\{\widetilde{W}_{j,t+\tau}^{(Y)}\}$ where $t = L_j - \tau - 1, ..., N - 1$ for $\tau < 0$.

4.1. Wavelet Cross-covariance

The formula for an approximate $100(1-2p)\%$ CI of the scale λ_j MODWT estimator of the wavelet cross-covariance $\tilde{\gamma}_{\tau,XY}(\lambda_j)$, starting from Equation (3), is provided; see also *Lindsay* et al. [1996]. We make use of the periodogram and the cross-periodogram to help estimate quantities of interest under the assumption of $\tau = 0$. First, we use the periodogram $\widehat{S}_{j,X}^{(p)}(\cdot)$ of $\{\widetilde{W}_{j,t}^{(X)}\}$ as the estimator of $S_{j,X}(\cdot)$, and similarly for $\widehat{S}_{j,Y}^{(p)}(\cdot)$ of $\{\widetilde{W}_{j,t}^{(Y)}\}$. Next, we define the biased estimator of the autocovariance sequence associated with the scale λ_j MODWT coefficients of $\{X_t\}$ by

$$\hat{s}_{j,m,X}^{(p)} \equiv \frac{1}{\widetilde{N}_j} \sum_{l=L_j-1}^{N-1-|m|} \widetilde{W}_{j,l}^{(X)} \widetilde{W}_{j,l+|m|}^{(X)},$$

A similar definition applies to $\{\hat{s}_{j,m,Y}^{(p)}\}$, the biased estimator of the autocovariance sequence associated with the scale λ_j MODWT coefficients $\{\widetilde{W}_{j,t+m}^{(Y)}\}$. Second, we use the cross-periodogram $\widehat{S}_{j,XY}^{(p)}(\cdot)$ of $\{\widetilde{W}_{j,t}^{(X)}\}$ and $\{\widetilde{W}_{j,t}^{(Y)}\}$, as the estimator of $S_{j,XY}(\cdot)$, and the corresponding biased estimator of the cross covariance sequence associated with the scale λ_j MODWT coefficients by

$$\widehat{C}_{j,m,XY}^{(p)} \equiv \frac{1}{\widetilde{N}_j} \sum_{l} \widetilde{W}_{j,l}^{(X)} \widetilde{W}_{j,l+m}^{(Y)},$$

where the summation goes from $l = L_j - 1, \ldots, N - m - 1$ for $m \geq 0$ and from $l = L_j - m - 1, \ldots, N - 1$ for $m < 0$.

We can use Parseval's relation to develop an estimate of the large sample variance for the MODWT-based estimator of the wavelet cross-covariance (Equation (3)) using the autocovariance and cross-covariance sequences of the MODWT coefficients. Specifically, the integral of the product of the periodograms is determined from the autocovariance sequences of $\{\widetilde{W}_{j,t}^{(X)}\}$ and $\{\widetilde{W}_{j,t}^{(Y)}\}$ via

$$\int_{-1/2}^{1/2} \widehat{S}_{j,X}^{(p)}(f)\widehat{S}_{j,Y}^{(p)}(f)\,df = \hat{s}_{j,0,X}^{(p)}\hat{s}_{j,0,Y}^{(p)} + 2\sum_{m=1}^{\widetilde{N}_j-1} \hat{s}_{j,m,X}^{(p)}\hat{s}_{j,m,Y}^{(p)},$$

and the integral of the squared cross periodogram from the cross covariance sequence of $\{\widetilde{W}_{j,t}^{(X)}, \widetilde{W}_{j,t}^{(Y)}\}$ via

$$\int_{-1/2}^{1/2} \left[\widehat{S}_{j,YX}^{(p)}(f)\right]^2 df = \sum_{m=-(\widetilde{N}_j-1)}^{\widetilde{N}_j-1} \left[\widehat{C}_{j,m,XY}^{(p)}\right]^2.$$

Hence, an estimate for the large sample variance of the MODWT estimator of the wavelet cross-covariance is given by

$$\widetilde{\mathcal{V}}_j \equiv \frac{\hat{s}_{j,0,X}^{(p)}\hat{s}_{j,0,Y}^{(p)}}{2} + \sum_{m=1}^{\widetilde{N}_j-1} \hat{s}_{j,m,X}^{(p)}\hat{s}_{j,0,Y}^{(p)} + \frac{1}{2}\sum_{m=-(\widetilde{N}_j-1)}^{\widetilde{N}_j-1} \left[\widehat{C}_{j,0,XY}^{(p)}\right]^2. \tag{5}$$

The estimator $\widetilde{\mathcal{V}}_j$ is unbiased when $\tau = 0$ [*Whitcher*, 1998]. Under the assumption that the spectral estimates are close to the true values, an approximate $100(1-2p)\%$ confidence interval for $\gamma_{XY}(\lambda_j)$ is

$$\left[\, \tilde{\gamma}_{XY}(\lambda_j) - \Phi^{-1}(1-p)\sqrt{\frac{\widetilde{\mathcal{V}}_j}{\widetilde{N}_j}}\,,\quad \tilde{\gamma}_{XY}(\lambda_j) + \Phi^{-1}(1-p)\sqrt{\frac{\widetilde{\mathcal{V}}_j}{\widetilde{N}_j}}\,\right],$$

where $\Phi^{-1}(p)$ is the $p \times 100\%$ percentage point for the standard normal distribution.

4.2. Wavelet Cross-correlation

We now use the large sample theory developed in Section 3.4 to construct an approximate CI for the MODWT estimator of the wavelet cross-correlation. Given the non-normality of the correlation coefficient for small sample sizes, a nonlinear

transformation is sometimes required – Fisher's z-transformation [*Fisher*, 1915; *Kotz, Johnson, and Read*, 1982, Volume 3]. Let

$$h(\rho) \equiv \frac{1}{2}\log\left(\frac{1+\rho}{1-\rho}\right) = \tanh^{-1}(\rho)$$

define the transformation. For the estimated correlation coefficient $\hat{\rho}$, based on n independent samples, $\sqrt{n-3}(h(\hat{\rho}) - h(\rho))$ has approximately a $N(0,1)$ distribution.

An approximate $100(1-2p)\%$ CI for $\rho_{XY}(\lambda_j)$ based on the MODWT is therefore

$$\left[\tanh\left\{h[\tilde{\rho}_{XY}(\lambda_j)] - \frac{\Phi^{-1}(1-p)}{\sqrt{\widehat{N}_j - 3}}\right\},\ \tanh\left\{h[\tilde{\rho}_{XY}(\lambda_j)] + \frac{\Phi^{-1}(1-p)}{\sqrt{\widehat{N}_j - 3}}\right\}\right]$$

where $\widehat{N}_j = N_j - L'_j$ and $L'_j = \lceil (L-2)(1-2^{-j}) \rceil$ is the number of DWT coefficients associated with scale λ_j. We are using the number of wavelet coefficients as if $\tilde{\rho}_{XY}(\lambda_j)$ had been computed using the DWT because, under the assumptions of Fisher's z-transformation, the denominator should consist of the number of independent samples used in constructing the correlation coefficient. If the autospectra and cross spectrum of the two processes $\{X_t, Y_t\}$ are slowly varying over each octave band of the DWT, the assumption of uncorrelated DWT coefficients is justified; see *McCoy and Walden* [1996] and the references contained therein. This property simply does not hold for the MODWT coefficients. If an equivalent degrees of freedom argument were available for the wavelet cross-covariance, as was used when establishing CIs for the wavelet variance based on the MODWT [*Percival*, 1995], this could be used instead of $\widehat{N}_j$.

5. Application

5.1. Introduction

The relationship between ENSO events and the MJO is a topic which could benefit by using wavelet techniques. To investigate how these two atmospheric phenomena interact, we analyze two time series. The first one being the Southern Oscillation Index

(SOI) [*Walker*, 1928], which is an indicator of ENSO and usually defined to be the difference between monthly averages of the station pressure series from climate stations at Darwin, Australia (130.8°E, 12.4°S) and Tahiti, French Polynesia (149°W, 14°S).

We deviate slightly from the usual definition of the SOI by introducing a daily version of it. We obtained daily pressure readings from Darwin, Australia, and Tahiti, French Polynesia, starting in 1 June 1957 and continuing through 31 December 1992 ($N = 12,998$) and differenced them; see Figure 1. The distance of the stations from the equator is apparent in the strong annual component in the time series. The measurements in the summer and winter of 1983 appear to be higher than those in adjacent years. This approximately corresponds to a large ENSO event in the early 1980s. We also obtained daily station pressure readings from Truk Island (7.4°N, 151.8°W) as an indicator of the MJO. This series also exists from 1 June 1957 to 31 December 1992; see Figure 1. Unlike the SOI, there is no apparent annual trend given its close proximity to the equator. Missing values in both series were replaced by one-step-ahead predictions from an ARIMA(3,1,0) model applied to the series [*Jones*, 1980].

5.2. Time-Domain and Spectral Analysis

Here we analyze the SOI and Truk Island station pressure series using standard time and frequency domain techniques. The cross-correlation sequence is typically estimated by utilizing the periodogram-based estimates of the autocovariance sequences for $\{X_t\}$ and $\{Y_t\}$, and their cross-covariance sequence. The estimated cross-correlation sequence for the SOI and Truk Island series is shown in Figure 2. The maximum occurs at a lag of +1 days. We also observe the characteristic broad-band peak commonly found in atmospheric time series from this region, with a approximate range of 35–55 day lags.

A bivariate spectral analysis of these data (Figure 3) provides some insight into the

possible relationship between ENSO events and the MJO. A Parzen smoothing window was applied to the periodogram with the window parameter chosen such that the spectral window bandwidth was 0.0081 day^{-1}, as in *Madden and Julian* [1971]. The lag window co-spectrum between the SOI and Truk Island station pressure series exhibits a large peak at the lower frequencies, which include the annual and inter-annual cycles, and two distinct peaks (centered at 0.0163 day^{-1} and 0.0273 day^{-1}) in the frequency range of the MJO. We can test, at the α level of significance, the null hypothesis of zero mean squared coherence (MSC) by checking the estimated MSC, on a frequency by frequency basis, against $1 - \alpha^{2/(\nu-2)}$ and rejecting if the estimated MSC exceeds it [*Koopmans*, 1974, p. 284]. The parameter ν is the number of equivalent degrees of freedom associated with the spectral estimates; $\nu \approx 189$ using Table 269 in *Percival and Walden* [1993]. We see that both peaks are significant at the 5% and 1% levels for a broad range of frequencies.

5.3. Wavelet Analysis

Daily measurements allow us to apply the MODWT and analyze the sub-series which correspond to filtered series with approximate pass-band $1/2^{j+1} \leq |f| \leq 1/2^{j}$. Due to the approximate bandpass nature of the MODWT, with the approximation improving as the length of the wavelet filter increases, it is unnecessary to remove any annual or semiannual components (a similar argument is made when bandpass filtering atmospheric time series in *Anderson* et al. [1984]), which should be roughly captured in the λ_7 and λ_8 scales. The MJO is known to occur with periods of around 30–60 days. We therefore expect to see it in scale λ_5, associated with changes of 16 days and an approximate pass-band of $1/64 \leq |f| \leq 1/32$.

A partial MODWT ($J = 10$) was applied to each series using the Daubechies least asymmetric wavelet filter of length $L = 8$ – which we denote by LA(8). Figures 4 and 5 give the MODWT coefficients for the Truk Island station pressure series and SOI,

respectively. Each vector has been circularly shifted in order to obtain an approximate zero-phase filter, allowing us to align features across scales; see *Percival and Mofjeld* [1997] for more details. For the Truk Island series, we observe only a slight annual trend in the $\widetilde{\mathbf{W}}_8$ series and the large disruption in the early 1980s appears to primarily affect scales λ_7 through λ_{10}. The $\widetilde{\mathbf{W}}_5$ series, associated with frequencies in the range of the MJO, appears to fade in and out in magnitude with no apparent pattern. The SOI multiresolution analysis exhibits a strong annual trend where the disturbance in the early 1980s affects the scales λ_8 through λ_1. Again, the scale associated with the MJO $\widetilde{\mathbf{W}}_5$ exhibits numerous bursts across time.

Figure 6 shows the estimated wavelet correlation between the SOI and Truk station pressure series at a lag of zero days. The wavelet correlation appears to be significantly different from zero (in fact, positive) for all scales except λ_6 and λ_7. The significant correlation for scale λ_5, and larger magnitude with respect to neighboring scales, lends credibility to the hypothesis of an association between the fluctuations in ENSO activity and the MJO.

If we are to investigate a possible lead/lag relationship between the two series, then the wavelet cross-correlation must be estimated for various lags. Figure 7 shows the estimated wavelet cross-correlation between the SOI and Truk Island station pressure series. Confidence intervals (not displayed) may be computed from Section 4.2. The large positive peak in the first five scales is at a lag of 1 day for scales λ_1 and λ_2, a lag of 2 days for scales λ_3, a lag of 4 days for scale λ_4 and zero days for scale λ_5. The higher scales do not show any apparent trend when looking at lags up to ± 240 days.

There is an obvious asymmetry in the wavelet cross-correlation for scales λ_4 and higher. The analysis here was performed so that at a lag of $+1$ day, the SOI time series leads the Truk station pressure series. As already noted for scale λ_5, the largest positive cross-correlation occurs at lag zero. The largest negative cross-correlation is at a lag of 20 days, approximately half the period of the MJO, and the second largest positive

cross-correlation occurs at a lag of 41 days, approximately a full period of the MJO. Even though the SOI consists of a difference between two stations with different spatial locations, there is still a strong 40 day oscillation which is correlated (and in phase) with the Truk station pressure series. It is also interesting to note that the wavelet cross-correlation for the first three scales is essentially an odd function. A possible interpretation is that common short-term weather patterns are causing these small scale disturbances. In contrast, the wavelet cross-correlation for scales λ_6 and λ_7 are essentially even functions. Patterns in higher scales (lower frequencies) correspond to the annual and inter-annual trends.

Although direct comparison between Figure 7 and Figure 2 is not appropriate, because the wavelet correlation does not decompose the correlation between two stationary processes, the wavelet covariance does decompose the covariance between two time series. Since the wavelet correlation is simply the wavelet covariance standardized at each scale, the shape of each wavelet cross-correlation is the same even though the magnitudes are off. Hence, we may make a rough comparison between the two, keeping in mind the facts just stated.

The first obvious difference is the fact that usual cross-correlation is positive for all negative lags. Looking at Figure 7, we see that the wavelet cross-correlation for scales λ_9 and λ_{10} are all positive and contribute to this feature, whereas for positive lags they are close to zero and allow the annual scale (λ_8) to dominate. The two dips on either side of the peak at a lag of +1 days is the superposition of the first six scales in Figure 7. The subsequent peak around a lag of +40 days is a result of the anti-correlation for scales λ_5 and λ_6 reducing the annual cross-correlation component (λ_8) for smaller lags. This leads to a different interpretation than what is seen by looking at the usual cross-correlation sequence. The correlation structure, when applied to all scales simultaneously, results in a quite complex looking cross-correlation sequence. When broken up with the wavelet transform a few simple, yet distinct, patterns appear which may be associated with

known atmospheric phenomena.

6. Discussion

We have introduced a new analysis technique for bivariate Gaussian time series which utilizes the MODWT. Certain nonstationary time series, with dth order stationary backward differences, are easily handled by this methodology. As in the univariate case with the wavelet variance, natural estimators of the cross-covariance and cross-correlation are defined. The wavelet cross-covariance and wavelet cross-correlation "decompose" their classical counterparts on a scale by scale basis. Thus, complicated patterns of association between time series are broken down into several much simpler patterns – each one associated with a physical time scale. With any good statistical analysis a measure of variability is also required, and the central limit theorems here enable approximate confidence intervals to be calculated.

A thorough analysis between the Southern Oscillation Index and a station pressure series from Truk Island was performed in order to gain insight into potential interactions between ENSO events and the MJO. Whereas conventional time and frequency domain techniques provide results which are difficult to interpret, the wavelet cross-correlation nicely displays how the association between the two processes changes with scale. Short-term weather patterns (changes of 1, 2 and 4 days) exhibit symmetric wavelet cross-correlations. The fifth scale, associated with the MJO, shows that the SOI (an indicator of ENSO activity) is correlated with Truk Island station pressure series (an indicator of the MJO) and they are roughly in phase. This scale exhibits the strongest magnitude correlations when compared with scales shorter than those associated with the semi-annual and annual frequencies.

References

Anderson, J. R., D. E. Stevens, and P. R. Julian (1984). Temporal variations of the tropical 40–50 day oscillation. *Monthly Weather Review 112*(12), 2431–2438.

Brillinger, D. R. (1979). Confidence intervals for the crosscovariance function. In *Mathematical Statistics*, Volume 5 of *Selecta Statistica Canadiana*, pp. 1–16. Hamilton, Ontario: McMaster University Printing Services.

Brillinger, D. R. (1981). *Time Series: Data Analysis and Theory*. Holden-Day Series in Time Series Analysis. San Francisco: Holden-Day. Expanded edition.

Daubechies, I. (1992). *Ten Lectures on Wavelets*, Volume 61 of *CBMS-NSF Regional Conference Series in Applied Mathematics*. Philadelphia: Society for Industrial and Applied Mathematics.

Fisher, R. A. (1915). Frequency distribution of the values of the correlation coefficient in samples from an indefinitely large population. *Biometrika 10*, 507–521.

Foufoula-Georgiou, E. and P. Kumar (Eds.) (1994). *Wavelets in Geophysics*, Volume 4 of *Wavelet Analysis and its Applications*. San Diego: Academic Press, Inc.

Gray, B. M. (1988). Seasonal frequency variations of the 40–50 day oscillation. *Journal of Climatology 8*, 511–519.

Hudgins, L., C. A. Friehe, and M. E. Mayer (1993). Wavelet transforms and atmospheric turbulence. *Physical Review Letters 71*(20), 3279–3282.

Hudgins, L. H. (1992). *Wavelet Analysis of Atmospheric Turbulence*. Ph. D. thesis, University of California, Irvine.

Jones, R. H. (1980). Maximum likelihood fitting of ARMA models to time series with missing observations. *Technometrics 22*(3), 389–395.

Koopmans, L. H. (1974). *The Spectral Analysis of Time Series*. New York. Academic Press.

Kotz, S., N. L. Johnson, and C. B. Read (Eds.) (1982). *Encyclopedia of Statistical Sciences*. New York: Wiley.

Kuhnel, I. (1989). Spatial and temporal variations in Australo–Indonesian region cloudiness. *International Journal of Climatology 9*(4), 395–405.

Kumar, P. (1996). Role of coherent structures in the stochastic-dynamic variability of precipitation. *Journal of Geophysical Research-Atmospheres 101*(D21), 26393–26404.

Kumar, P. and E. Foufoula-Georgiou (1994). Wavelet analysis in geophysics: An introduction. See *Foufoula-Georgiou and Kumar* [1994], pp. 1–43.

Lindsay, R. W., D. B. Percival, and D. A. Rothrock (1996). The discrete wavelet transform and the scale analysis of the surface properties of sea ice. *IEEE Transactions on Geoscience and Remote Sensing 34*(3), 771–787.

Liu, P. C. (1994). Wavelet spectrum analysis and ocean wind waves. See *Foufoula-Georgiou and Kumar* [1994], pp. 151–166.

Madden, R. A. (1986). Seasonal variation of the 40–50 day oscillation in the tropics. *Journal of Atmospheric Science 43*(24), 3138–3158.

Madden, R. A. and P. R. Julian (1971). Detection of a 40–50 day oscillation in the zonal wind in the tropical pacific. *Journal of Atmospheric Science 28*, 702–708.

Madden, R. A. and P. R. Julian (1994). Observations of the 40–50 day tropical oscillation: A review. *Monthly Weather Review 122*(5), 814–837.

Mann, H. B. and A. Wald (1943). On stochastic limit and order relationships. *The Annals of Mathematical Statistics 14*, 217–226.

McCoy, E. J. and A. T. Walden (1996). Wavelet analysis and synthesis of stationary long-memory processes. *Journal of Computational and Graphical Statistics 5*(1), 26–56.

Percival, D. B. (1995). On estimation of the wavelet variance. *Biometrika 82*(3), 619–631.

Percival, D. B. and P. Guttorp (1994). Long-memory processes, the Allan variance and wavelets. See *Foufoula-Georgiou and Kumar* [1994], pp. 325–344.

Percival, D. B. and H. O. Mofjeld (1997). Analysis of subtidal coastal sea level fluctuations using wavelets. *Journal of the American Statistical Association 92*(439), 868–880.

Percival, D. B. and A. T. Walden (1993). *Spectral Analysis for Physical Applications: Multitaper and Conventional Univariate Techniques*. Cambridge: Cambridge University Press.

Percival, D. B. and A. T. Walden (1999). *Wavelet Methods for Time Series Analysis*. Cambridge: Cambridge University Press. Forthcoming.

Titchmarsh, E. C. (1939). *The Theory of Functions* (2 ed.). Oxford: Oxford University Press.

Torrence, C. and G. P. Compo (1998). A practical guide to wavelet analysis. *Bulletin of the American Meteorological Society 79*(1), 61–78.

Walker, G. T. (1928). World weather. *Monthly Weather Review 56*, 167–170.

Whitcher, B. (1998). *Assessing Nonstationary Time Series Using Wavelets*. Ph. D. thesis, University of Washington.

Received _____

Appendix A: Proofs of Theorems

Lemma 1 *For all $\epsilon > 0$, there exists a J_ϵ such that* $\left|\mathrm{Cov}\left\{\overline{V}_{J,t}^{(X)}, \overline{V}_{J,t}^{(Y)}\right\}\right| < \epsilon$ *for* $J > J_\epsilon$.

Proof of Lemma 1 For the orthonormal DWT $\sum_l g_{J,l}^2 = 1$ and by definition $\tilde{g}_{J,l} = g_{J,l}/2^{J/2}$. Therefore we have $\sum_l \tilde{g}_{J,l}^2 = 1/2^J$. Parseval's relation tells us that

$$\int_{-1/2}^{1/2} \widetilde{\mathcal{G}}_J(f)\, df = \int_{-1/2}^{1/2} \left|\widetilde{G}_J(f)\right|^2 \, df = \sum_{l=0}^{L_J-1} \tilde{g}_{J,l}^2 = \frac{1}{2^J}.$$

We know the amplitude spectrum $A_{XY}(f) \equiv |S_{XY}(f)|$ is a non-negative real valued function. Hence, if $A_{XY}(\cdot)$ is bounded by some finite number C, then for $J > J_\epsilon$,

$$\left|\mathrm{Cov}\left\{\overline{V}_{J,t}^{(X)}, \overline{V}_{J,t}^{(Y)}\right\}\right| \le \int_{-1/2}^{1/2} \widetilde{\mathcal{G}}_J(f)\, |S_{XY}(f)| \, df = C \int_{-1/2}^{1/2} \widetilde{\mathcal{G}}_J(f)\, df = \frac{C}{2^J} < \epsilon.$$

If $A_{XY}(\cdot)$ cannot be bounded by any finite number C, there at least exists a constant C_ϵ such that $\int_{A_{XY}(f)\ge C_\epsilon} A_{XY}(f)\, df < \epsilon/2$, using a Lebesgue integral. A rough bound on the squared gain function of the scaling filter for Daubechies wavelets is $\widetilde{\mathcal{G}}_J(f) \le 1$, so for all $J > J_\epsilon$,

$$\begin{aligned}
\left|\int_{-1/2}^{1/2} \widetilde{\mathcal{G}}_J(f) S_{XY}(f)\, df\right| &\le \int_{A_{XY}(f)\ge C_\epsilon} \widetilde{\mathcal{G}}_J(f)\, |S_{XY}(f)| \, df + \int_{A_{XY}(f)<C_\epsilon} \widetilde{\mathcal{G}}_J(f)\, |S_{XY}(f)| \, df \\
&\le \int_{A_{XY}(f)\ge C_\epsilon} A_{XY}(f)\, df + C_\epsilon \int_{A_{XY}(f)<C_\epsilon} \widetilde{\mathcal{G}}_J(f)\, df \\
&\le \frac{\epsilon}{2} + C_\epsilon \int_{-1/2}^{1/2} \widetilde{\mathcal{G}}_J(f)\, df \le \frac{\epsilon}{2} + \frac{C_\epsilon}{2^J} < \epsilon.
\end{aligned}$$

□

Proof of Theorem 1 Without loss of generality, we set $\tau = 0$ and simply shift $\{\overline{W}_{j,t}^{(Y)}\}$ with respect to $\{\overline{W}_{j,t}^{(X)}\}$ to get $\tau \neq 0$. Because $\{\overline{W}_{j,t}^{(X)}\}$ and $\{\overline{W}_{j,t}^{(Y)}\}$ are obtained by filtering the processes $\{X_t\}$ and $\{Y_t\}$ with a Daubechies compactly supported wavelet filter of even length $L > 2d$, respectively, we know that $\{\overline{W}_{j,t}^{(X)}\}$ and $\{\overline{W}_{j,t}^{(Y)}\}$ are stationary processes with autospectra defined by $S_{j,X}(f) \equiv \widetilde{\mathcal{H}}_j(f) S_X(f)$ and $S_{j,Y}(f) \equiv \widetilde{\mathcal{H}}_j(f) S_Y(f)$ where $\widetilde{\mathcal{H}}_j(f) \equiv \widetilde{\mathcal{H}}(2^{j-1}f) \prod_{l=0}^{j-2} \widetilde{\mathcal{G}}(2^l f)$ is the squared gain

function for $\{\tilde{h}_j\}$. Note, the squared gain functions associated with unit scale for the wavelet and scaling filters are given by $\widetilde{\mathcal{H}}(f) \equiv |\widetilde{H}(f)|^2$ and $\widetilde{\mathcal{G}}(f) \equiv |\widetilde{G}(f)|^2$.

The covariance between $\{\overline{W}_{j,t}^{(X)}\}$ and $\{\overline{W}_{j,t}^{(Y)}\}$ is given by

$$\gamma_{XY}(\lambda_j) = \int_{-1/2}^{1/2} \widetilde{\mathcal{H}}_j(f) S_{XY}(f)\, df.$$

This is a straightforward generalization of the univariate case; see *Whitcher* [1998] for more details. The covariance between $\{\overline{V}_{j,t}^{(X)}\}$ and $\{\overline{V}_{j,t}^{(Y)}\}$ is given by

$$\text{Cov}\left\{\overline{V}_{J,t}^{(X)}, \overline{V}_{J,t}^{(Y)}\right\} = \int_{-1/2}^{1/2} \widetilde{\mathcal{G}}_J(f) S_{XY}(f)\, df,$$

where $\widetilde{\mathcal{G}}_J(f) \equiv \prod_{l=0}^{J-1} \widetilde{\mathcal{G}}(2^l f)$ is the squared gain function for $\{\tilde{g}_J\}$. Because of the following identity for squared gain functions $\widetilde{\mathcal{H}}(f) + \widetilde{\mathcal{G}}(f) = 1$ for all f [*Percival and Walden*, 1999, Sec. 4.3], we have

$$\text{Cov}\{X_t, Y_t\} = \int_{-1/2}^{1/2} \left[\widetilde{\mathcal{G}}(f) + \widetilde{\mathcal{H}}(f)\right] S_{XY}(f)\, df = \text{Cov}\left\{\overline{V}_{1,t}^{(X)}, \overline{V}_{1,t}^{(Y)}\right\} + \gamma_{XY}(\lambda_1),$$

and the case when $J = 1$ holds. We now proceed to prove the main assertion by induction. Assume the property holds for $J-1$; i.e.,

$$\text{Cov}\{X_t, Y_t\} = \text{Cov}\left\{\overline{V}_{J-1,t}^{(X)}, \overline{V}_{J-1,t}^{(Y)}\right\} + \sum_{j=1}^{J-1} \gamma_{XY}(\lambda_j).$$

So we have

$$\begin{aligned}
\text{Cov}\left\{V_{J-1,t}^{(X)}, V_{J-1,t}^{(Y)}\right\} &= \int_{-1/2}^{1/2} \left[\prod_{l=0}^{J-2} \widetilde{\mathcal{G}}(2^l f)\right] S_{XY}(f)\, df \\
&= \int_{-1/2}^{1/2} \left[\widetilde{\mathcal{G}}(2^{J-1} f) + \widetilde{\mathcal{H}}(2^{J-1} f)\right] \left[\prod_{l=0}^{J-2} \widetilde{\mathcal{G}}(2^l f)\right] S_{XY}(f)\, df \\
&= \int_{-1/2}^{1/2} \left[\widetilde{\mathcal{G}}_J(f) + \widetilde{\mathcal{H}}_J(f)\right] S_{XY}(f)\, df \\
&= \text{Cov}\left\{\overline{V}_{J,t}^{(X)}, \overline{V}_{J,t}^{(Y)}\right\} + \gamma_{XY}(\lambda_J).
\end{aligned}$$

The decomposition of covariance between $\{X_t, Y_t\}$ has now been established for a finite number of scales. From Lemma 1, as $J \to \infty$ the remaining covariance between the scaling coefficients goes to zero. Hence, the theorem is established.

□

Proof of Theorem 2 Without loss of generality, we set $\tau = 0$ and simply shift $\{\overline{W}_{j,t}^{(Y)}\}$ with respect to $\{\overline{W}_{j,t}^{(X)}\}$ to get $\tau \neq 0$. With $L > 2d$, both series of MODWT coefficients $\{\overline{W}_{j,t}^{(X)}\}$ and $\{\overline{W}_{j,t}^{(Y)}\}$ have zero mean. Square integrability of the autospectra implies that $\{s_{j,\tau,X}\} \longleftrightarrow S_{j,X}(\cdot)$ and $\{s_{j,\tau,Y}\} \longleftrightarrow S_{j,Y}(\cdot)$; i.e., the autocovariance sequences and autospectra are Fourier transform pairs. Because $L > 2d$, the squared gain function for Daubechies wavelet filters guarantees we have $S_{j,X}(0) = 0 = \sum_{\tau=-\infty}^{\infty} s_{j,\tau,X}$. A similar statement holds for $\{\widetilde{W}_{j,t}^{(Y)}\}$ and, therefore, $\{s_{j,\tau,X}\}$ and $\{s_{j,\tau,Y}\}$ are absolutely summable.

Let $S_{j,XY}(f) \equiv \widetilde{\mathcal{H}}_j(f) S_{XY}(f)$ denote the MODWT filtered cross spectrum. From the magnitude squared coherence being bounded by unity, and using the Cauchy–Schwarz inequality, we know that

$$\begin{aligned} \int_{-1/2}^{1/2} |S_{j,XY}(f)|^2 \, df &\leq \int_{-1/2}^{1/2} S_{j,X}(f) S_{j,Y}(f) \, df \\ &\leq \left(\int_{-1/2}^{1/2} S_{j,X}^2(f) \, df \int_{-1/2}^{1/2} S_{j,Y}^2(f) \, df \right)^{1/2} < \infty. \end{aligned}$$

So the cross-covariance sequence and cross spectrum associated with scale λ_j are also a Fourier pair and, again, by using a Daubechies wavelet filters with $L > 2d$, we have $S_{j,XY}(0) = 0$. Therefore, the cross-covariance sequence for $\{\overline{W}_{j,t}^{(X)}, \overline{W}_{j,t}^{(Y)}\}$ is absolutely summable.

We first note that the MODWT estimate of the wavelet covariance $\tilde{\gamma}_{XY}(\lambda_j)$ is essentially a sample mean for the time series $\overline{W}_{j,t}^{(XY)} \equiv \overline{W}_{j,t}^{(X)} \overline{W}_{j,t}^{(Y)}$ (cf. Equation (1)). This process also has an absolutely summable cumulant sequence by Theorem 2.9.1 of *Brillinger* [1981, p. 38]. Then Theorem 4.4.1 of *Brillinger* [1981, p. 94] tells us that $\tilde{\gamma}_{XY}(\lambda_j)$ is asymptotically normal with mean $\gamma_{XY}(\lambda_j)$ and large sample variance given by $\widetilde{N}_j^{-1} S_{j,(XY)}(0)$, where $S_{j,(XY)}(0)$ is the spectral density for $\overline{W}_{j,t}^{(XY)}$ evaluated at $f = 0$.

□

Derivation of Equation 2 Since we are exclusively interested in Gaussian processes, $S_{j,(XY)}(0)$ may be re-expressed as a function of the auto and cross spectra of the wavelet coefficients $\{W_{j,l}^{(X)}\}$ and $\{W_{j,l}^{(Y)}\}$. The variance of the estimated MODWT wavelet covariance at scale λ_j can be computed directly via

$$\begin{aligned}
\mathrm{Var}\{\tilde{\gamma}_{XY}(\lambda_j)\} &= \frac{1}{\widetilde{N}_j^2} \sum_{l=L_j-1}^{N-1} \sum_{m=L_j-1}^{N-1} \mathrm{Cov}\left\{\widetilde{W}_{j,l}^{(X)}\widetilde{W}_{j,l}^{(Y)}, \widetilde{W}_{j,m}^{(X)}\widetilde{W}_{j,m}^{(Y)}\right\} \\
&= \frac{1}{\widetilde{N}_j} \sum_{\tau=-(\widetilde{N}_j-1)}^{\widetilde{N}_j-1} \left(1 - \frac{|\tau|}{\widetilde{N}_j}\right) \mathrm{Cov}\left\{\widetilde{W}_{j,l}^{(X)}\widetilde{W}_{j,l}^{(Y)}, \widetilde{W}_{j,l+\tau}^{(X)}\widetilde{W}_{j,l+\tau}^{(Y)}\right\} \\
&\equiv \frac{1}{\widetilde{N}_j} \sum_{\tau=-(\widetilde{N}_j-1)}^{\widetilde{N}_j-1} \left(1 - \frac{|\tau|}{\widetilde{N}_j}\right) s_{j,\tau,XY}\,, \qquad \text{(A1)}
\end{aligned}$$

where $s_{j,\tau,XY}$ is the autocovariance sequence for the product of the scale λ_j MODWT coefficients with respect to $\{X_t\}$ and $\{Y_t\}$.

Using the Isserlis theorem and properties of the Fourier transform, the spectrum of $\{Z_t\}$ at $f = 0$ is $S_Z(0) = \int_{-1/2}^{1/2} S_U(f)S_V(f)\,df + \int_{-1/2}^{1/2} S_{UV}^2(f)\,df$ [*Whitcher*, 1998]. Since we have the Fourier relationship $\{s_{\tau,Z}\} \longleftrightarrow S_Z(\cdot)$, we necessarily have $S_Z(0) = \sum_{\tau=-\infty}^{\infty} s_{\tau,Z}$, when $f = 0$. Re-examining Equation (A1) and utilizing Cesàro summability [*Titchmarsh*, 1939, p. 411], we can say

$$\begin{aligned}
\lim_{\widetilde{N}_j\to\infty} \widetilde{N}_j \,\mathrm{Var}\{\tilde{\gamma}_{XY}(\lambda_j)\} &= \lim_{\widetilde{N}_j\to\infty} \sum_{\tau=-(\widetilde{N}_j-1)}^{\widetilde{N}_j-1} \left(1 - \frac{|\tau|}{\widetilde{N}_j}\right) s_{j,\tau,XY} \\
&= \sum_{\tau=-\infty}^{\infty} s_{j,\tau,XY} = S_{j,(XY)}(0),
\end{aligned}$$

where

$$S_{j,(XY)}(0) = \int_{-1/2}^{1/2} S_{j,X}(f)S_{j,Y}(f)\,df + \int_{-1/2}^{1/2} S_{j,XY}^2(f)\,df$$

□

Proof of Theorem 3 Since $L > 2d$, we have that both sets of wavelet coefficients $\{\widetilde{W}_{j,t}^{(X)}\}$ and $\{\widetilde{W}_{j,t}^{(Y)}\}$ have mean zero. Let us define $A_{j,t} \equiv [\widetilde{W}_{j,t}^{(X)}]^2$, $B_{j,t} \equiv [\widetilde{W}_{j,t}^{(Y)}]^2$, and

$C_{j,t} \equiv \widetilde{W}_{j,t}^{(X)} \widetilde{W}_{j,t}^{(Y)}$, and subsequently define their sample means

$$\begin{aligned}
\overline{A}_j &\equiv \frac{1}{\widetilde{N}_j} \sum_{t=L_j-1}^{N-1} A_{j,t} = \tilde{\nu}_X^2(\lambda_j), \\
\overline{B}_j &\equiv \frac{1}{\widetilde{N}_j} \sum_{t=L_j-1}^{N-1} B_{j,t} = \tilde{\nu}_Y^2(\lambda_j), \quad \text{and} \\
\overline{C}_j &\equiv \frac{1}{\widetilde{N}_j} \sum_{t=L_j-1}^{N-1} C_{j,t} = \tilde{\gamma}_{XY}(\lambda_j).
\end{aligned}$$

The vector-valued process $\{A_{j,t}, B_{j,t}, C_{j,t}\}$ has an absolutely summable joint cumulant sequence by Theorem 2.9.1 of *Brillinger* [1981, p. 38]. Hence, from Theorem 4.4.1 of *Brillinger* [1981, p. 94] the vector of sample means $\{\overline{A}_j, \overline{B}_j, \overline{C}_j\}$ are asymptotically normally distributed with mean vector $\{\nu_X^2(\lambda_j), \nu_Y^2(\lambda_j), \gamma_{XY}(\lambda_j)\}$, and large sample variance given by $\widetilde{N}_j^{-1} \mathbf{S}_{j,ABC}(0)$, where $\mathbf{S}_{j,ABC}(\cdot)$ is the 3×3 spectral matrix for $\{A_{j,t}, B_{j,t}, C_{j,t}\}$.

The MODWT estimator of the wavelet correlation $\tilde{\rho}_{XY}(\lambda_j)$ is essentially a function of these sample means $g(\overline{A}_j, \overline{B}_j, \overline{C}_j)$, where $g(x,y,z) \equiv z/\sqrt{xy}$. Appealing to *Mann and Wald* [1943], we have that $\tilde{\rho}_{XY}(\lambda_j)$ is asymptotically normally distributed with mean $\rho_{XY}(\lambda_j)$ and large sample variance

$$\widetilde{N}_j^{-1} \, \dot{g}\left(\nu_X^2(\lambda_j), \nu_Y^2(\lambda_j), \gamma_{XY}(\lambda_j)\right)^T \, \mathbf{S}_{j,ABC}(0) \, \dot{g}\left(\nu_X^2(\lambda_j), \nu_Y^2(\lambda_j), \gamma_{XY}(\lambda_j)\right) \qquad \text{(A2)}$$

where $\dot{g}(\cdot,\cdot,\cdot)$ is the gradient of $g(\cdot,\cdot,\cdot)$. Now let us re-express Equation (A2) into the desired result using the fact that we are only interested in Gaussian processes. Because we are evaluating $\mathbf{S}_{j,ABC}(\cdot)$ at $f = 0$, it is in fact a symmetric matrix of the form

$$\mathbf{S}_{j,ABC}(0) = \begin{bmatrix} S_{j,AA}(0) & S_{j,AB}(0) & S_{j,AC}(0) \\ S_{j,AB}(0) & S_{j,BB}(0) & S_{j,BC}(0) \\ S_{j,AC}(0) & S_{j,BC}(0) & S_{j,CC}(0) \end{bmatrix},$$

where the elements of the matrix are

$$\begin{aligned}
S_{j,AA}(0) &= 2\int_{-1/2}^{1/2} S_{j,X}^2(f)\,df, \quad S_{j,BB}(0) = 2\int_{-1/2}^{1/2} S_{j,Y}^2(f)\,df, \\
S_{j,CC}(0) &= \int_{-1/2}^{1/2} S_{j,X}(f)S_{j,Y}(f)\,df + \int_{-1/2}^{1/2} S_{j,XY}^2(f)\,df, \\
S_{j,AB}(0) &= 2\int_{-1/2}^{1/2} S_{j,XY}(f)S_{j,YX}(f)\,df, \\
S_{j,AC}(0) &= 2\int_{-1/2}^{1/2} S_{j,X}(f)S_{j,YX}(f)\,df, \quad \text{and} \\
S_{j,BC}(0) &= 2\int_{-1/2}^{1/2} S_{j,Y}(f)S_{j,YX}(f)\,df.
\end{aligned}$$

The gradient is explicitly given by

$$\dot{g}\left(\nu_X^2(\lambda_j), \nu_Y^2(\lambda_j), \gamma_{XY}(\lambda_j)\right) = \left[-\frac{\gamma_{XY}(\lambda_j)}{2\nu_X^2(\lambda_j)\sqrt{\nu_X^2(\lambda_j)\nu_Y^2(\lambda_j)}} \;\; -\frac{\gamma_{XY}(\lambda_j)}{2\nu_Y^2(\lambda_j)\sqrt{\nu_X^2(\lambda_j)\nu_Y^2(\lambda_j)}} \;\; \frac{1}{\sqrt{\nu_X^2(\lambda_j)\nu_Y^2(\lambda_j)}} \right]^T,$$

and, through matrix multiplication and application of Parseval's relation to each auto and cross spectra in $\mathbf{S}_{j,ABC}(0)$, we may express Equation (A2) as

$$\begin{aligned}
\frac{1}{\widetilde{N}_j} \sum_{\tau=-(\tilde{N}_j-1)}^{\tilde{N}_j-1} \Bigg\{ & \frac{\gamma_{XY}^2(\lambda_j)}{4\nu_X^6(\lambda_j)\nu_Y^2(\lambda_j)}\, 2s_{j,\tau,X}^2 + \frac{\gamma_{XY}^2(\lambda_j)}{2\nu_X^4(\lambda_j)\nu_Y^4(\lambda_j)}\, 2C_{j,\tau,XY}C_{j,\tau,YX} \\
& + \frac{\gamma_{XY}^2(\lambda_j)}{4\nu_X^2(\lambda_j)\nu_Y^6(\lambda_j)}\, 2s_{j,\tau,Y}^2 + \frac{1}{\nu_X^2(\lambda_j)\nu_Y^2(\lambda_j)} \left(s_{j,\tau,X}s_{j,\tau,Y} + C_{j,\tau,XY}^2\right) \\
& - \frac{\gamma_{XY}(\lambda_j)}{\nu_X^4(\lambda_j)\nu_Y^2(\lambda_j)}\, 2s_{j,\tau,X}C_{j,\tau,YX} - \frac{\gamma_{XY}(\lambda_j)}{\nu_X^2(\lambda_j)\nu_Y^4(\lambda_j)}\, 2s_{j,\tau,Y}C_{j,\tau,YX} \Bigg\}.
\end{aligned}$$

Each of the autocovariance terms are equivalent to the wavelet autocovariance for scale λ_j (defined by letting $X_t = Y_t$ in Equation (1)) and each cross-covariance term is equivalent to the wavelet cross-covariance for scale λ_j. This yields the desired result.

□

List of Figures

1. Station pressure series for Truk Island (7.4°N, 151.8°W) and the Southern Oscillation Index. The "staggered" look of the Truk Island series prior to 1971 is the result of rounding to the nearest millibar.

2. Estimated cross-correlation sequence for the Southern Oscillation Index and Truk Island station pressure series for lags up to ±240 days.

3. Estimated lag window co-spectrum and magnitude squared coherence (MSC) between the Southern Oscillation Index and Truk Island station pressure series. A Parzen lag window, with spectral window bandwidth 0.0081 day^{-1}, was applied to the periodogram. The dotted and dashed lines correspond to the 5% and 1% levels of significance test for non-zero MSC, respectively.

4. MODWT coefficients for the Truk Island station pressure series using the LA(8) wavelet filter. The wavelet coefficient vectors $\widetilde{\mathbf{W}}_1, \widetilde{\mathbf{W}}_2, \ldots, \widetilde{\mathbf{W}}_{10}$ are associated with variations on scales of $1, 2, \ldots, 1024$ days and the scaling coefficient vector $\widetilde{\mathbf{V}}_{10}$ is associated with variations of 2048 days or longer.

5. MODWT coefficients for the daily Southern Oscillation Index using the LA(8) wavelet filter. The wavelet and scaling coefficients have the same interpretation as in Figure 4.

6. MODWT estimated wavelet correlation between the Southern Oscillation Index and Truk Island station pressure series.

7. MODWT estimated wavelet cross-correlation between the Southern Oscillation Index and Truk Island station pressure series for lags up to ±240 days. Confidence intervals may be computed from Section 4.2. The positive peak in the fifth scale λ_5 is at a lag of 0 days.

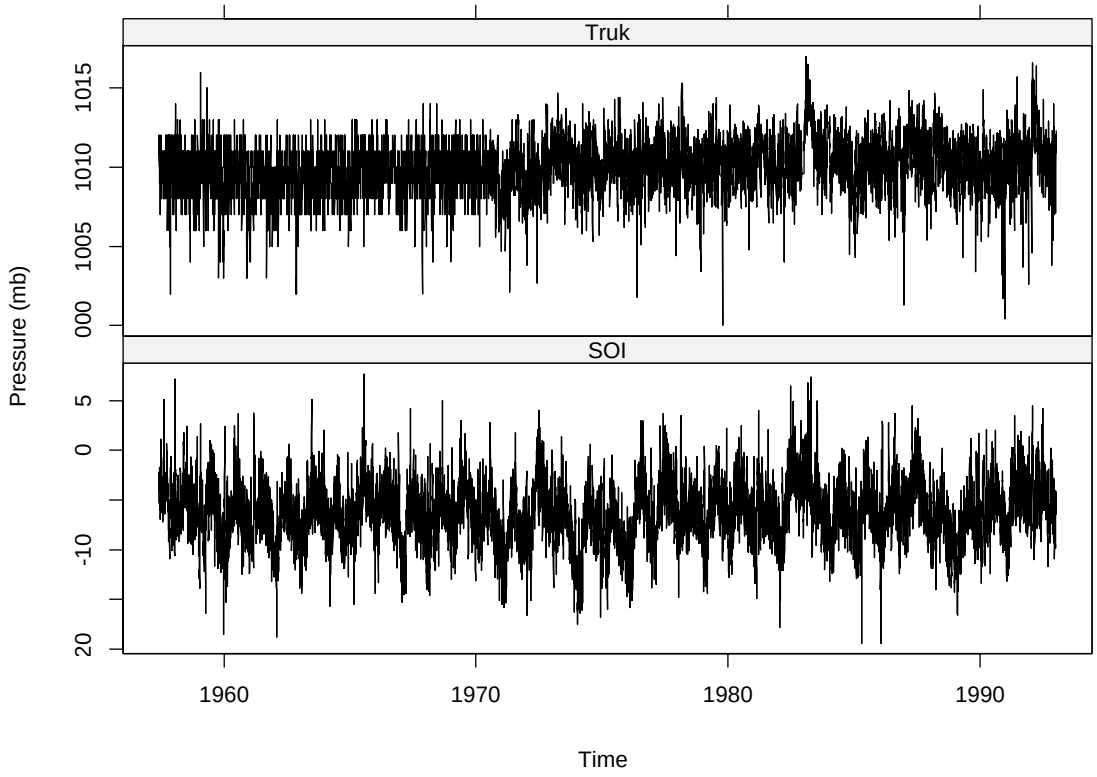

Figure 1.

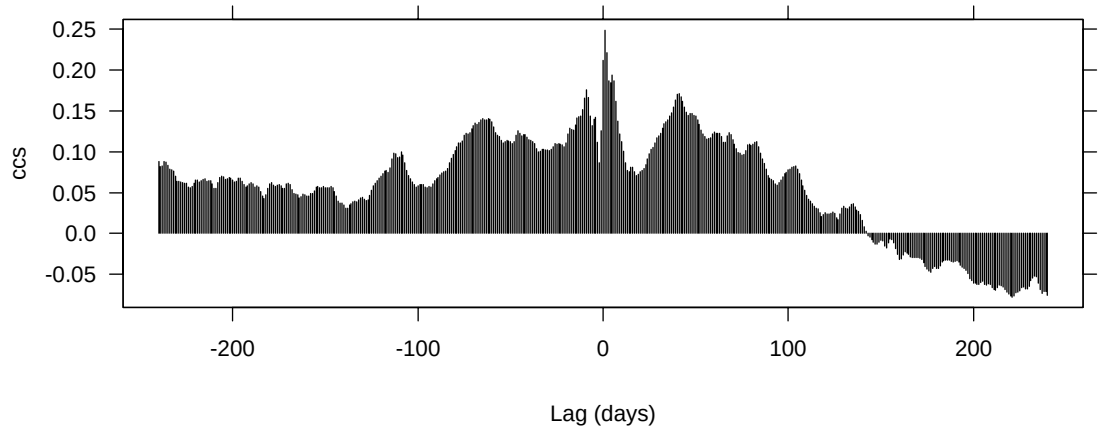

Figure 2.

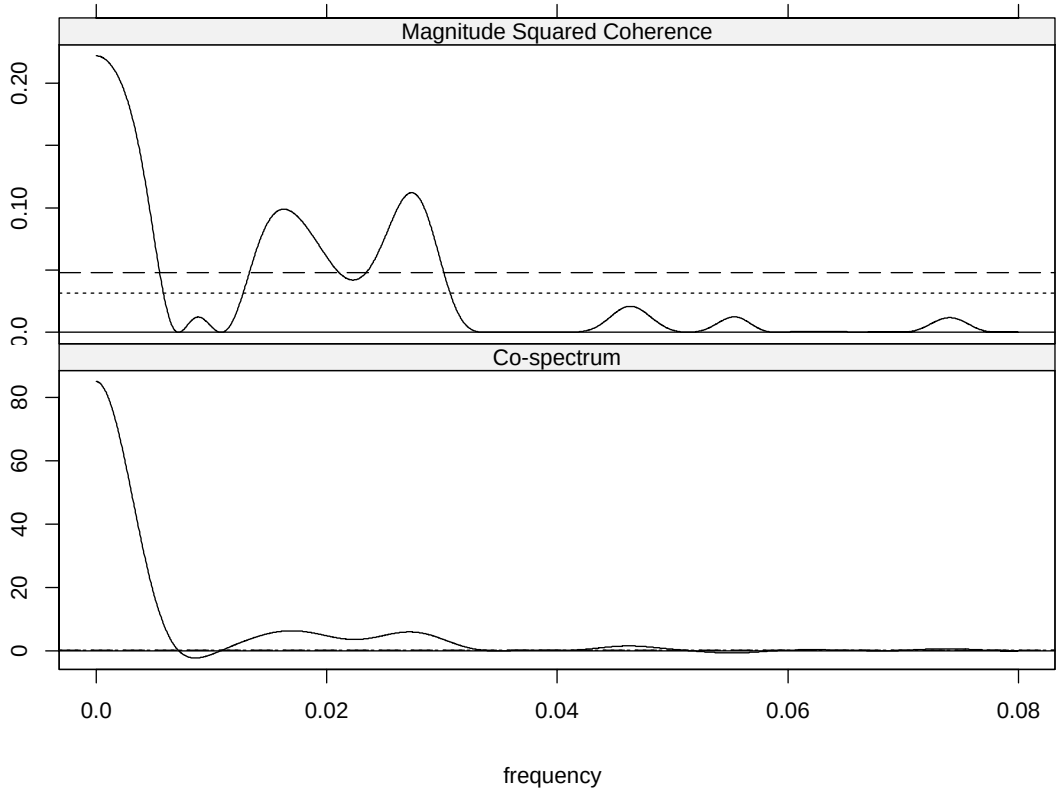
Magnitude Squared Coherence
0.20
0.10
0.0
Co-spectrum
80
60
40
20
0
0.0
0.02
0.04
0.06
0.08
frequency

Figure 3.

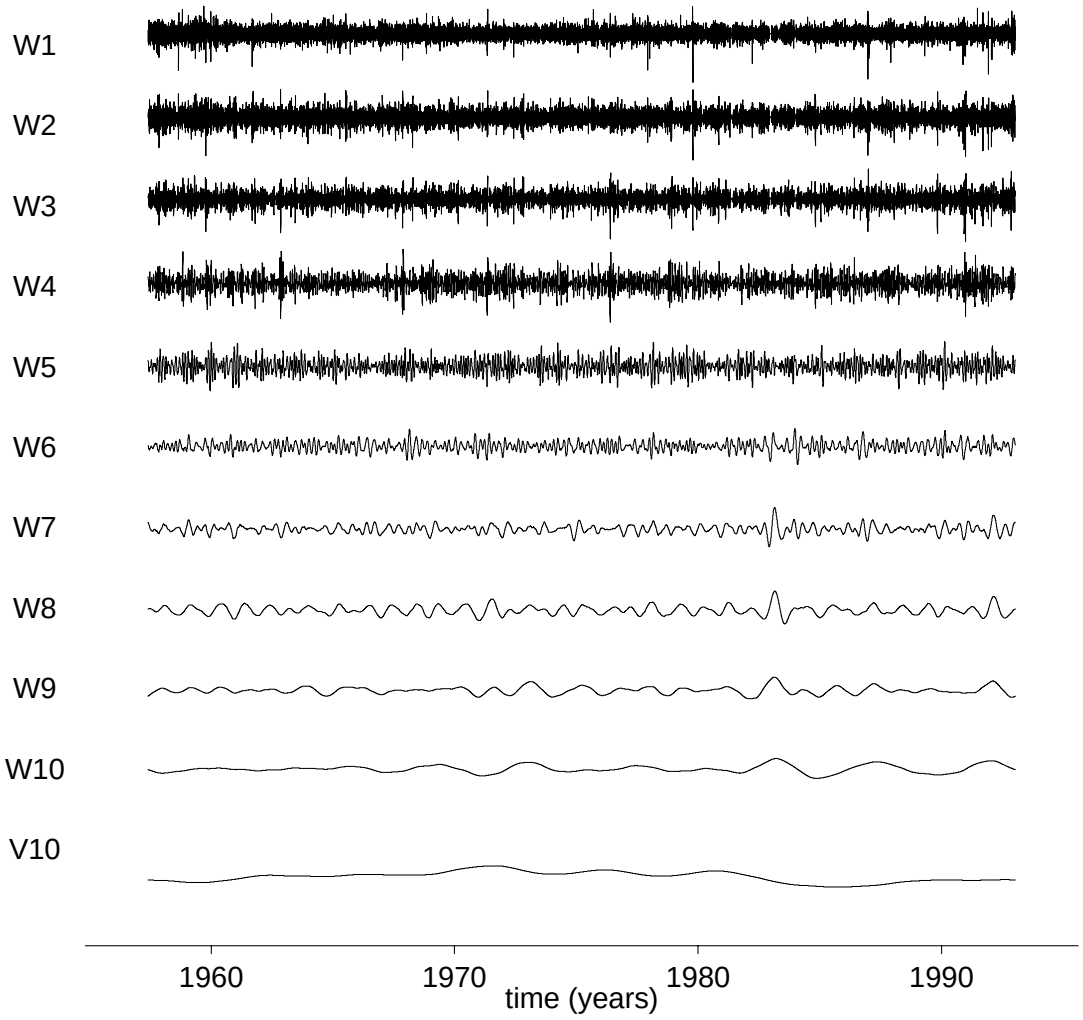

Figure 4.

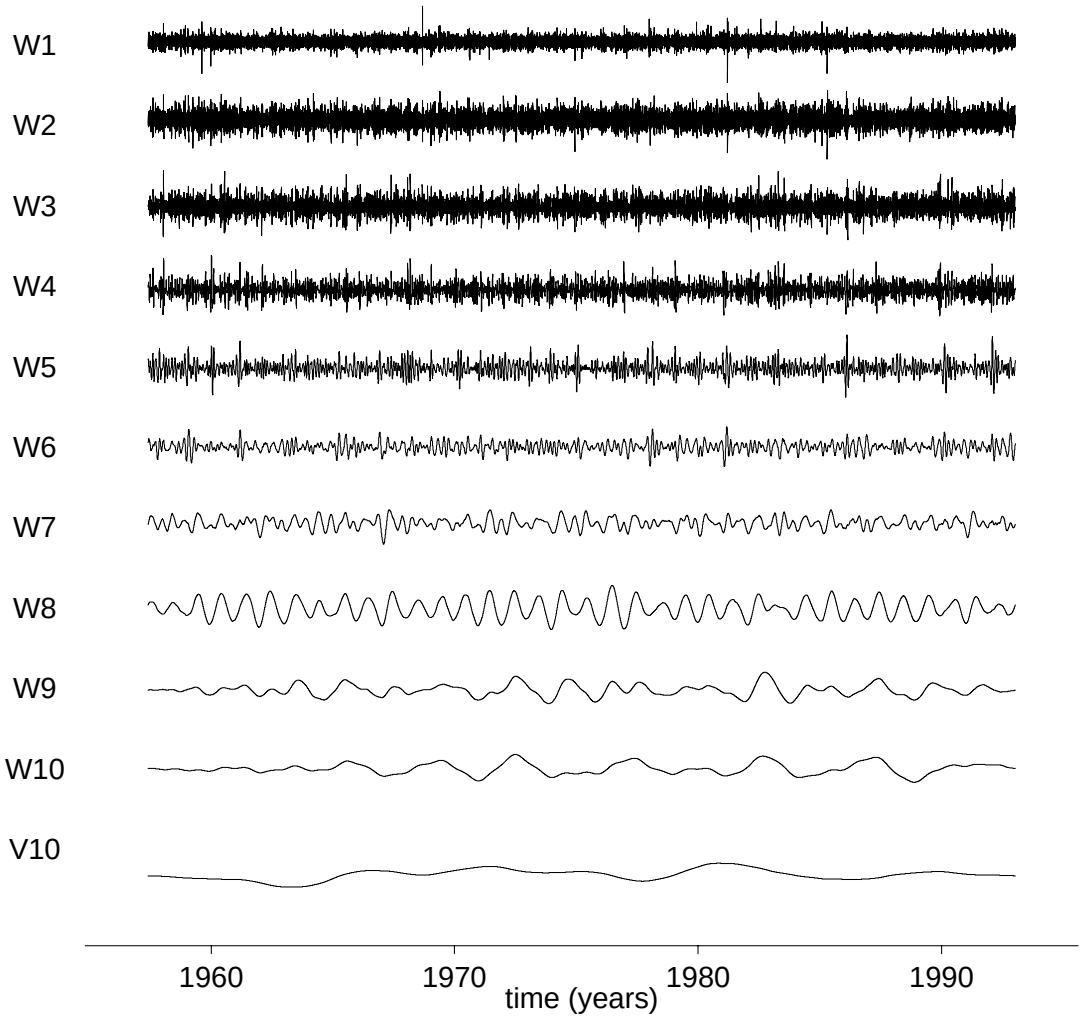

Figure 5.

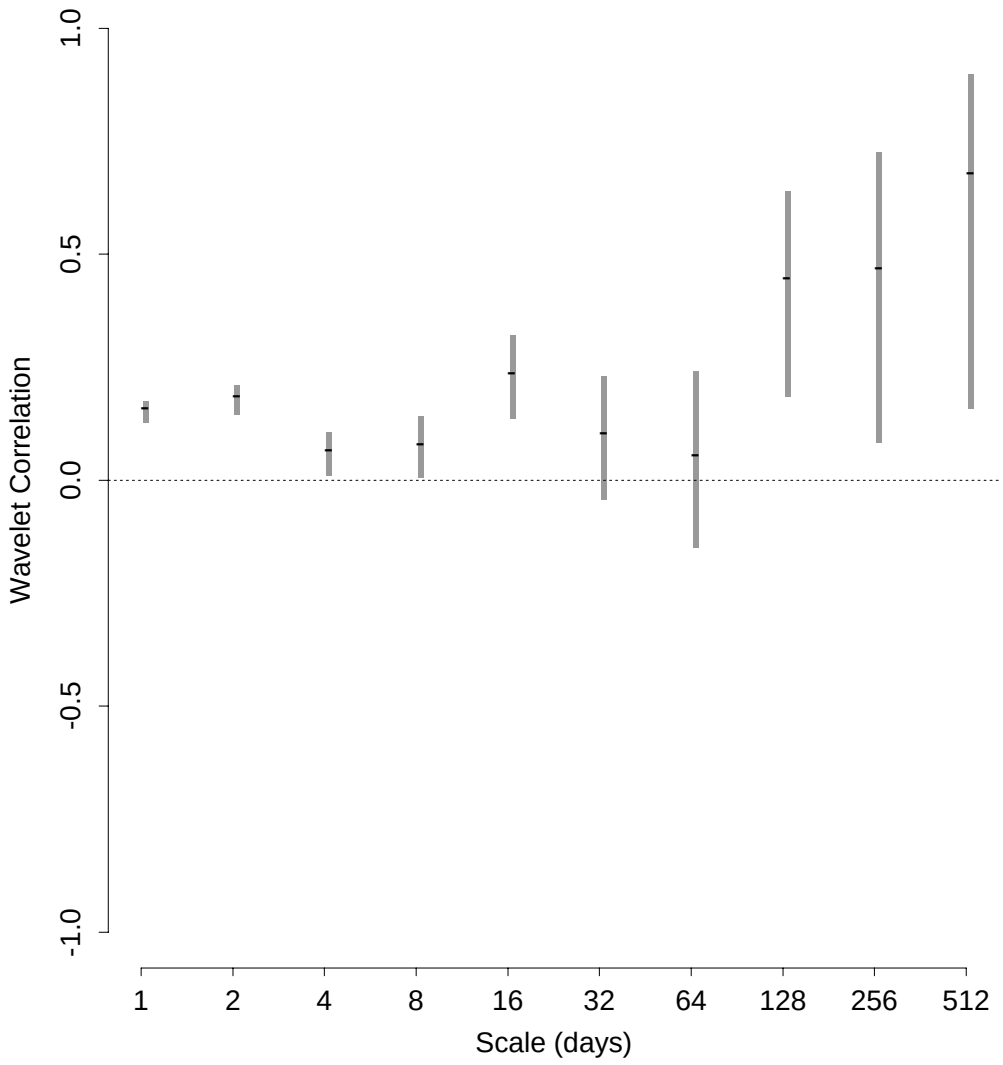
Wavelet Correlation
1.0
0.5
0.0
-0.5
-1.0
1
2
4
8
16
32
64
128
256
512
Scale (days)

Figure 6.

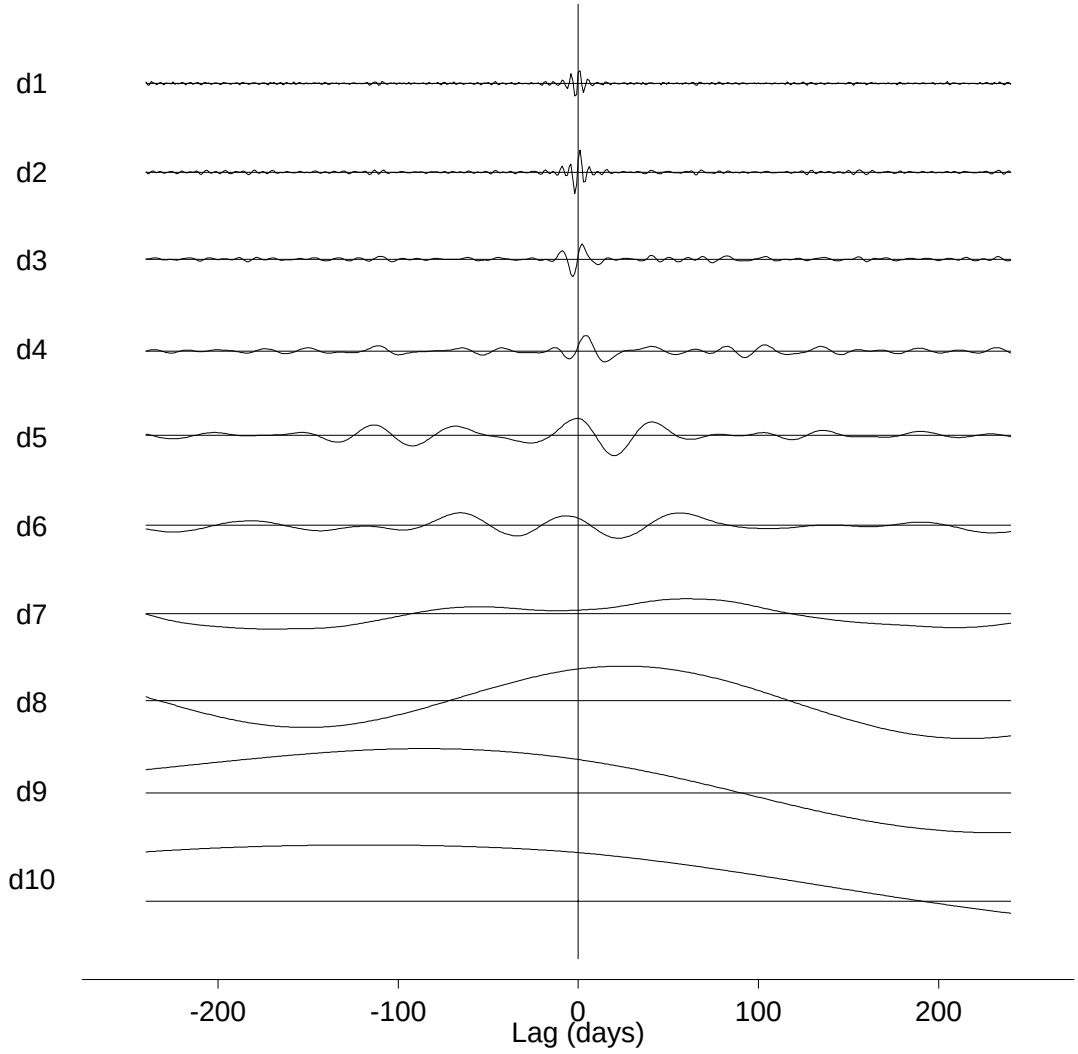

Figure 7.